Science of the Total Environment 823 (2022) 153636

Contents lists available at ScienceDirect

Science of the Total Environment

journal homepage: www.elsevier.com/locate/scitotenv

Effects of different carbon sources on methane production and the methanogenic communities in iron rich flooded paddy soil

Dan Luo [a,b,c], Yaying Li [a,b], Huaiying Yao [a,b,d,*], Stephen J. Chapman [e]

[a] Key Laboratory of Urban Environment and Health, Institute of Urban Environment, Chinese Academy of Sciences, Xiamen 361021, People's Republic of China
[b] Zhejiang Key Laboratory of Urban Environmental Processes and Pollution Control, Ningbo Urban Environment Observation and Research Station-NUEORS, Institute of Urban Environment, Chinese Academy of Sciences, Ningbo 315800, People's Republic of China
[c] University of Chinese Academy of Sciences, Beijing 100049, People's Republic of China
[d] Research Center for Environmental Ecology and Engineering, School of Environmental Ecology and Biological Engineering, Wuhan Institute of Technology, Wuhan 430073, People's Republic of China
[e] The James Hutton Institute, Craigiebuckler, Aberdeen AB15 8QH, UK

HIGHLIGHTS

- The methanogenic capacity of glucose and starch were stronger than acetate.
- Methanosarcinales and Methanobacteriales were mainly responsible for CH_4 production.
- The type and abundance of methanogens changed with the incubation time.
- *mcrA* gene copies positively correlated with the reduction of Fe(III).

GRAPHICAL ABSTRACT

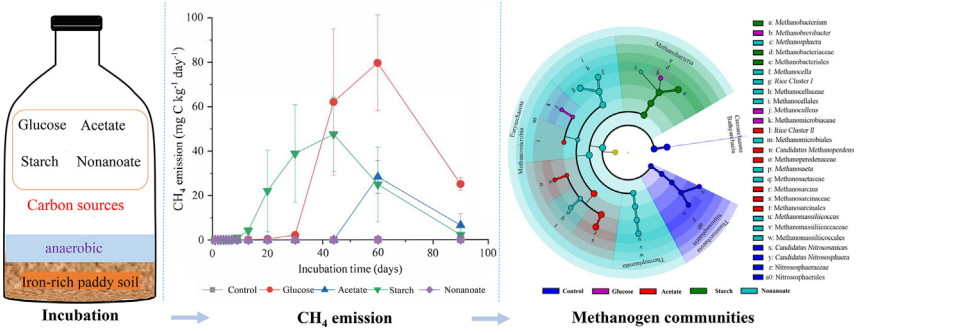

ARTICLE INFO

Article history:
Received 26 December 2021
Received in revised form 25 January 2022
Accepted 29 January 2022
Available online 4 February 2022

Editor: Jay Gan

Keywords:
Organic matter
Methanogen
High-throughput sequencing
Rice paddy
Iron reduction

ABSTRACT

Various carbon sources as substrates and electron donors can produce methane via different metabolic pathways. In particular, the methane produced by rice cultivation has a severe impact on climate change. However, how Fe^{3+}, the most abundant oxide in paddy soil, mediates the methanogenesis of different carbon sources is unknown. In this study, we investigated the effect of four carbon sources with different chain lengths (acetate, glucose, nonanoate, and starch) on CH_4 production and associated methanogens in iron-rich paddy soil over 90 days of anaerobic incubation. We found that glucose and starch were the more preferential substrates for liberating methane compared to acetate, and the rate was also faster. Nonanoate was unable to support methane production. Methanosarcinales and Methanobacteriales were the most predominant methanogenic archaea as shown by 16S rRNA gene sequencing, though their abundance changed over time. Additionally, a significantly higher content of iron-reducing bacteria was observed in the glucose and starch treatments, and it was significantly positively correlated with the copy number of the methanogenic *mcrA* gene. Together, we confirmed the methanogenic capacity of different carbon sources and their related microorganisms. We also showed that iron oxides play a central role in regulating methane emissions from paddy soils and need more attention to be paid to them.

1. Introduction

Methane (CH_4) is considered an important greenhouse gas. It has a global warming potential that is 84-fold greater than carbon dioxide (CO_2) over a 20-year period, and its continuous increase in the atmosphere

* Corresponding author at: Key Laboratory of Urban Environment and Health, Institute of Urban Environment, Chinese Academy of Sciences, Xiamen 361021, People's Republic of China.
E-mail address: hyyao@iue.ac.cn (H. Yao).

http://dx.doi.org/10.1016/j.scitotenv.2022.153636

is a global climate threat (Pachauri et al., 2014). Rice is one of the most important crops that feeds more than half of the world's population (Xu et al., 2020a). However, rice paddies are the largest source of anthropogenic CH_4 emissions and contribute 7 to 17% of the global methane sources (Su et al., 2015). It is generally believed that CH_4 is produced by the decomposition of organic carbon in strictly anaerobic soils and sediments (Gütlein et al., 2018). The CH_4 emission in paddy soil is regulated by microbial processes, including the balance between CH_4-producing archaea (methanogens) and CH_4-consuming bacteria (methanotrophs) (Liechty et al., 2020).

Iron is the fourth most abundant element, representing 4.2% of Earth's crust (Lanquar et al., 2005). The biogeochemical cycle of iron is closely linked to the cycling of carbon, nitrogen, and other elements (Bryce et al., 2018). Insoluble Fe^{3+} is the most common form of iron in natural habitats and influences electron transport processes as the most abundant mineral oxide in flooded anaerobic paddy habitats (Wandersman and Delepelaire, 2004; Weber et al., 2006). However, the influence of C compounds within the soil on CH_4 production from soil organic carbon (SOC) decomposition has been little studied and results so far are inconclusive. In our recent study, we found that iron oxides could effectively promote methane oxidation by iron-reducing bacteria (Luo et al., 2021). In addition, Fe^{3+} can act as a conductor in direct interspecies electron transfer (DIET) and therefore affect methanogenesis (Summers et al., 2010). Likewise, earlier studies pointed out that Fe^{3+} as an electron acceptor in flooded paddy fields can inhibit CH_4 emissions through its reduction to Fe^{2+}, but the complex physical environment makes it difficult to quantify the interrelationship between the two processes (Hanke et al., 2013). Gwon et al. (2018) found that the addition of Fe^{3+} decreased the abundance of methanogens in a paddy field, thus reducing CH_4 emissions. For this phenomenon, some researchers believe that iron reducers compete with methanogenic archaea for electron acceptors, i.e., the carbon source of the reaction substrate, thereby inhibiting the growth of methanogens (Marquart et al., 2019; Xu et al., 2020b). Furthermore, Lovley et al. (2004) indicated that the transition process of Fe^{3+}/Fe^{2+} has a specific impact on the soil electron transfer and organic carbon utilization, but the effect of the Fe^{3+} reduction process on the retention and decomposition of the carbon source is still unclear (Peng et al., 2015). In addition, Chen et al. (2020) simply stated that iron plays dual roles in promoting and inhibiting SOC decomposition due to its structure and nature.

All known methanogens belong to the strictly anaerobic phylum Euryarchaeota, domain archaea, and are divided into seven distinct orders: Methanosarcinales, Methanocellales, Methanobacteriales, Methanococcales, Methanomicrobiales, Methanomassiliicoccales, and Methanopyrales (Borrel et al., 2014). Methanogens fall into three metabolically distinct lineages depending on the substrate used: hydrogenotrophic, acetoclastic, and methylotrophic (Liu and Whitman, 2008). Some studies have found that SOC content mainly influenced the rate of CH_4 production and that CH_4 emissions increase with higher SOC degradation (Guérin et al., 2008; Kosugi et al., 2020). On the one hand, the carbon sources in flooded rice fields provide substrates for soil methanogens, and on the other hand, it promotes the decline of soil redox potential (Eh) and forms suitable conditions for the proliferation of methanogens (Rago et al., 2015). Methanogenic rate varies depending on the carbon source. For example, cellulose as a carbon source effectively promoted CH_4 emissions in peatlands, followed by glucose and acetate, and the degradation of acetate was the last (Bachoon and Jones, 1992). Meanwhile, Bridgham and Richardson (1992) found that glucose also can effectively promote CH_4 production in peatlands, while acetate inhibited CH_4 production. In addition, Peng et al. (2015) indicated that glucose significantly increased the cumulative CH_4 fluxes and revealed that Fe^{3+} reduction is vital in regulating the carbon cycle in paddy soils.

Currently, most studies usually focus on the response of straw and biochar as the substrate for CH_4 emission (Nan et al., 2020; Fu et al., 2021). Little is known about how foundational carbon sources affect CH_4 emission in paddy soil and requires further research. Considering the ubiquity and criticality of iron oxides in paddy fields system, we added four carbon sources with different chain lengths to an iron-rich paddy soil for flooded anaerobic incubation. The effect of carbon sources on CH_4 emission from iron rich paddy soils was investigated by measuring the dynamic changes of CH_4 and CO_2 emissions and the values of physicochemical factors. Furthermore, the community composition and abundance of archaea and bacteria were investigated using Illumina MiSeq high-throughput sequencing and quantitative PCR.

2. Materials and methods

2.1. Soil sampling and microcosm setup

The soil used for this experiment was sampled from the surface layer (0 to 20 cm) at a rice paddy field of Ningbo city, Zhejiang province, China in August 2019 (29°47′N, 121°22′E). Mean annual temperature and precipitation are 17.8 °C and 2020 mm, respectively. The specific sampling process was as described in (Luo et al., 2021). Soil samples were air-dried, homogenized, passed through a 2 mm sieve, and divided into two parts: one part was stored at 4 °C for soil physicochemical analysis and the other stored at −20 °C for the later experiment. The soil pH, organic carbon, total nitrogen, phosphorus, potassium, and HCl-extractable Fe were 5.5, 24.6, 4.8, 0.6, 8.7 and 1.52 g kg^{-1}, respectively.

We set up an anaerobic microcosm by adding 15 g of air-dried soil to sterile 120 ml serum bottles and mixed in sterile anaerobic distilled water at a ratio of 1:1.5 (*w/v*). Each bottle was amended with 5 g C kg^{-1} dry soil and with five treatments: (i) Control (the negative control without addition of carbon), (ii) Glucose, (iii) Acetate, (iv) Starch, (v) Nonanoate, with three replicates. Then, homogeneously mixed with the soil slurries, sealed with sterile neoprene septa, secured by an aluminum cap, and flushed with He gas until an anaerobic environment was formed, all anaerobic serum bottles were incubated at 25 °C in the dark for 90 days.

2.2. Gas and physicochemical properties measurements

The headspace gases in the serum bottles were sampled (about 100 μl) at 1, 2, 3, 4, 5, 6, 7, 9, 13, 20, 30, 44, 60, and 90 days for the measurement of CH_4 and CO_2 concentration by using an Agilent 7890A gas chromatograph (Palo Alto, CA, USA) equipped with a flame ionization detector (FID) and thermal conductivity detector (TCD). The temperatures of the injection port, detector and oven were 250, 250 and 60 °C, respectively. On days 1, 44, and 90, the soil physicochemical properties were measured. Soil pH was measured with a pH meter (soil/water ratio of 1:2.5). Soil Eh was measured using an Ag/AgCl electrode (Thermo Fisher Scientific, MA, USA). Soil dissolved organic carbon (DOC) was determined by a total organic carbon analyzer (Vario TOC, Germany). Soil microbial carbon (MBC) was measured by the fumigation–extraction method (Vance et al., 1987). Soil ammonium (NH_4^+-N) and nitrate (NO_3^--N) were determined using an autoanalyser (SEAL-AA3, Germany). Available phosphorus (AP) was analyzed by the molybdenum-antimony color method (Crouch and Malmstadt, 1967). Available potassium (AK) was determined by the flame photometry method (Lazcano et al., 2008). The concentration of Fe^{3+} and Fe^{2+} were measured using a ferrozine method (Achtnich et al., 1995). Fe^{2+} and total Fe concentrations were measured directly, and Fe^{3+} concentration was calculated by subtracting Fe^{2+} concentration from the total Fe concentrations.

2.3. DNA extraction and quantitative PCR analysis

Soil slurry samples at 1, 44, and 90 days were freeze-dried and extracted for total DNA using the FastDNA® SPIN Kit for Soil (MP Biomedicals, Solon). DNA concentration and quality were determined by a NanoDrop 2000 UV–vis spectrophotometer (Thermo Fisher Scientific, MA, USA). Real-time quantitative PCR (qPCR) was performed with a Light Cycler Roche 480 instrument (Roche Molecular Systems, Switzerland). The primer pairs McrA159F (5'-AAAGTGCGGAGCAGCAATCACC-3′) and McrA345R (5′ -TCGTCCCATTCCTGCTGCATTGC-3′) were used to quantify the methyl coenzyme M reductase (*mcrA*) gene (Vaksmaa et al., 2017). The primer

pairs cmo182F (5′- TCACGTTGACGCCGATCC-3′) and cmo568R (5'-GCAC ATACTCCATCCCCATC-3′) were used to quantify the partial CH_4 monooxygenase (*pmoA*) gene (Luesken et al., 2011). Sterile distilled water was used as a negative control. The standard curve was established using a 10-fold serial dilution of standard plasmid DNA. The standard DNA concentration for the *mcrA* gene was 4.26×10^9 copies·μl^{-1} and 5.20×10^9 copies·μl^{-1} for the *pmoA* gene. The qPCR mixtures were 20 μl, containing 10 μl 2× GoTaq® qPCR Master Mix (Promega), 0.4 μl of each primer, 2 μl of 10-fold diluted DNA template, and 7.2 μl of nuclease free water. The PCR conditions were 50 °C for 2 min, 95 °C for 5 min, followed by 40 cycles of 95 °C for 30 s, 56 °C for 40 s and 72 °C for 45 s, and then 72 °C elongation for 5 min. PCR amplification efficiencies of 87–92% were obtained for the *mcrA* gene and 82–91% for the *pmoA* gene, and the correlation coefficient (R^2) values were greater than 0.99.

2.4. Miseq sequencing of 16S rRNA gene

DNA samples were transported on dry ice to the Majorbio Bio-Pharm Technology Co., Ltd. (Shanghai, China) for MiSeq sequencing of 16S rRNA gene amplicons. Amplification of archaeal 16S rRNA gene targeted the V4–V5 regions used the universal primers Arch524F (5'-TGYCAGCCGCCGCGGT AA-3′) and Arch958R (5'-YCCGGCGTTGAVTCCAATT-3′) (Liu et al., 2016). For the V3–V4 regions of bacterial 16S rRNA gene, primers 338F (5'-ACTC CTACGGGAGGCAGCAG-3′) and 806R (5'-GGACTACHVGGGTWTCTAAT-3′) were used (Caporaso et al., 2011). Sequencing was performed on Illumina's MiSeq-PE250 platform. The raw sequences were deposited into the NCBI Sequence Read Archive (SRA) database with accession number PRJNA 706862.

2.5. Statistical analysis

Daily CH_4 flux was calculated as follows:

$$F = \rho \times V/m \times dc/dt \times 273/(273 + T) \times 12/16$$

Daily CO_2 flux was calculated as follows:

$$F = \rho \times V/m \times dc/dt \times 273/(273 + T) \times 12/44$$

where F (mg C kg^{-1} day^{-1}) is the CH_4 or CO_2 flux; ρ is the density of CH_4 (0.717 kg m^{-3}) or CO_2 (1.977 kg m^{-3}) at standard temperature and pressure (STP); V (m^3) is the headspace volume of the serum bottle; m (kg) is the dry soil weight of the serum bottle; dc/dt (ppm d^{-1}) is the changed concentration of CH_4 or CO_2 in the unit time (d); T is the incubation temperature.

All general statistical analyses were conducted using SPSS 26.0 (SPSS, Inc., Chicago, IL). The differences between treatments were analyzed using the one-way analysis of variance (ANOVA), and Duncan's tests at a probability of $P < 0.05$ was regarded as being statistically significant. The correlations between different parameters were assessed using Pearson's correlation analysis. Possible chimeras of the sequences were checked using the QIIME platform (version 1.9.0). Downstream processing and Operational Taxonomic Units (OTUs) were clustered at 97% identity (Edgar, 2013). Taxonomy was assigned to each sequence using the Ribosomal Database Project (RDP) Classifier (version 2.2, 80% confidence threshold) based on the SILVA 132 reference database (https://www.arb-silva.de/) (Quast et al., 2012). Alpha diversity indices (Shannon, Chao1) were calculated using alpha_diversity.py in QIIME. For estimating community dissimilarities, the Bray–Curtis dissimilarity was calculated using beta_diversity.py. Principal Coordinate of Analysis (PCoA) plot was performed using the vegan package and ade4 package in R based on the Bray-Curtis distances at the OTU level. Significant differences were tested by using a multivariate PERMANOVA, and permutations were set to 999. Redundancy analysis (RDA) was carried out using the vegan package in R based on the order taxonomy level of archaea. Archaeal biomarkers were identified using the LEfSe method (Logarithmic LDA > 3; alpha value < 0.05) (Segata et al., 2011). The correlations between archaeal genus composition and physicochemical parameters, including functional genes, environmental factors, and gas emissions, were analyzed using a heatmap.

3. Results

3.1. Fluxes of CH_4 and CO_2

The influence of carbon sources on CH_4 and CO_2 emissions are shown in Fig. 1. In the absence of added carbon, no CH_4 emissions were observed throughout the entire incubation period. CH_4 emissions were significantly increased with glucose, acetate, and starch addition ($P < 0.05$), but with no apparent effect after the application of nonanoate (Fig. 1A). With starch, the CH_4 emissions increased rapidly from day 13 and began to decrease from day 44. With glucose, the CH_4 emissions mainly started from day 44, and the maximum emission was 79.56 mg C kg^{-1} day^{-1} on day 60, followed by a sharp decline. However, with acetate, significant CH_4 was not emitted until day 60, and then decreased by day 90. Regarding the accumulation of CH_4 emissions, the ranking was glucose>starch>acetate, with the nonanoate and control treatments close to zero (Fig. 1B). With glucose, the CO_2 emissions mainly occurred in the first 7 days, reaching a maximum of 1150 mg C kg^{-1} day^{-1} and then decreasing, with a short secondary emission process apparent at day 44 (Fig. 1C). The overall trend of the CO_2 emissions with the starch treatment was similar to that of the glucose treatment, but the emission in the early stage of glucose addition was significantly higher than that of starch ($P < 0.05$). Moreover, the trend of CO_2 emissions with control, acetate, and nonanoate in the early stage of incubation were the same and very low (< 28.5 mg C kg^{-1} day^{-1}), but began to rise slightly with the acetate addition after day 44. The cumulative CO_2 emissions of the different carbon sources exhibited similar trends with the cumulative CH_4 emissions (Fig. 1D). The relationship between environmental factors and CH_4 emission has been identified by the correlation analysis (Table 1). CH_4 emissions were significantly negatively correlated with the concentration of Fe^{3+} ($P < 0.001$), and positively correlated with the relative abundance of the *mcrA* gene ($P < 0.001$).

3.2. mcrA and pmoA genes copy numbers and soil physicochemical properties

We determined the copy number of the genes methanogen *mcrA* and methanotroph *pmoA* with different carbon sources at 1, 44, and 90 days (Fig. 2). On the first day of anaerobic incubation, we found a small but significant increase in the number of *mcrA* gene copies with glucose, acetate, and starch compared to the control ($P < 0.05$). The number of *mcrA* gene copies in all treatments increased to varying degrees from day 44. On days 44 and 90, there was a significant increase in the copy number of the *mcrA* gene between the treatments of glucose and starch compared to other treatments ($P < 0.05$). Also, the copy number of the *mcrA* gene was significantly increased with acetate compared to the control on days 90 ($P < 0.05$). Meanwhile, the copy number of the *pmoA* gene with different treatments did not show an obvious pattern during the incubation. On days 1 and 44, the copy number of the *pmoA* gene with the acetate treatment was the highest, and there was a significant difference from the other treatments ($P < 0.05$). However, on days 90, the copy number of the control was the highest, and there was a significant difference with the carbon source treatments ($P < 0.05$). Pearson analysis (Table 1) explains the relationship between the *mcrA* and *pmoA* genes and other environmental variables. Among the explanatory variables, CH_4 emissions and Fe^{2+} had significantly positive effects ($P < 0.001$), while pH, DOC, and Fe^{3+} had significantly negative effects ($P < 0.001$) with the *mcrA* gene. At the same time, pH and CH_4 emissions had significant effects on the number of *pmoA* gene copies with the coefficients 0.32, and − 0.32, respectively. Additionally, the concentration of Fe^{3+} was significantly positively correlated with pH, DOC and NH_4^+ ($P < 0.001$), and negatively correlated with AK ($P < 0.001$).

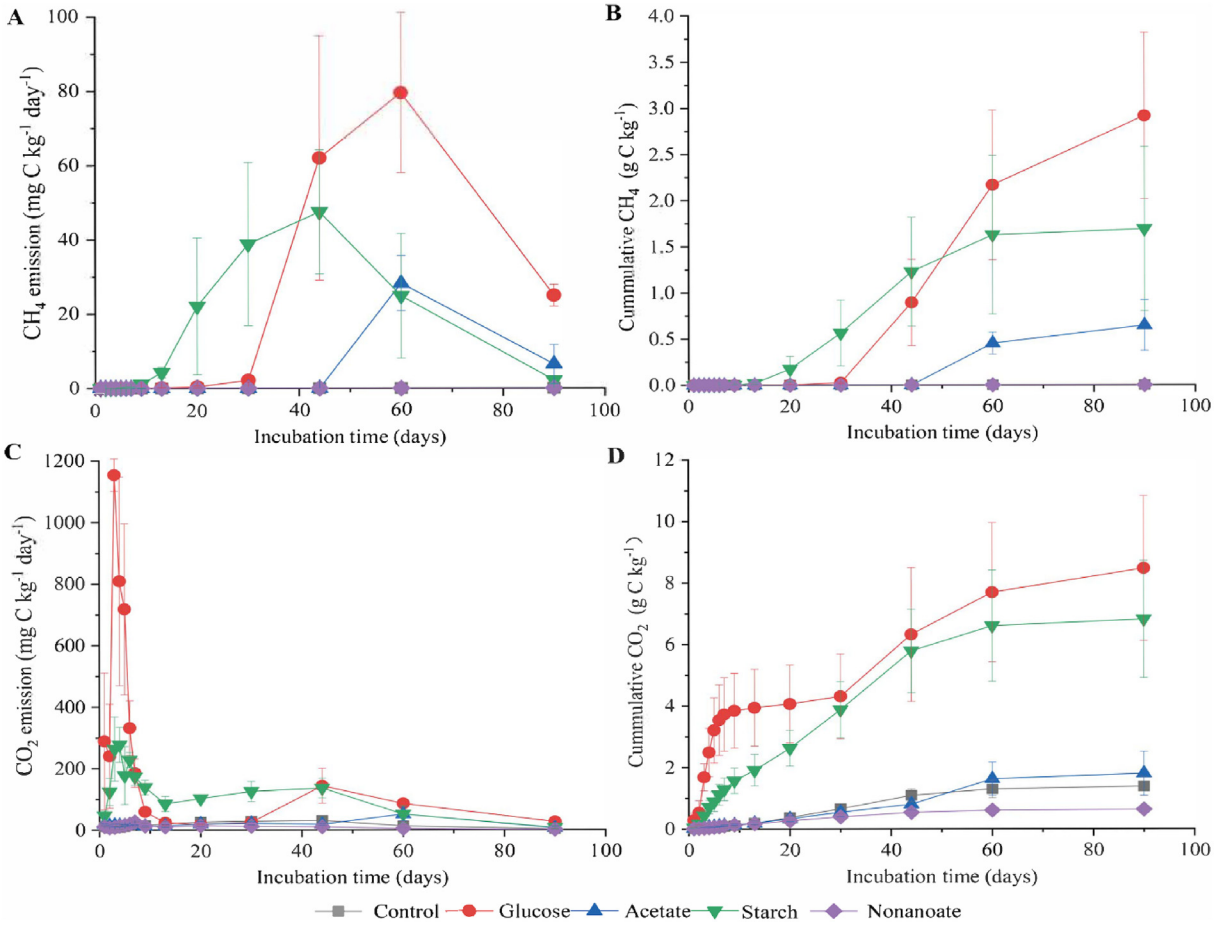

Fig. 1. The variation in CH_4 and CO_2 concentrations with time with different carbon sources. The error bars show standard error (n = 3).

3.3. Microbial community structure with different carbon sources

Microbial community analysis was carried out through 16S rRNA gene sequencing, and the relative distribution of bacteria and archaea were derived from the OTUs at three incubation times (1, 44, and 90 days). A total of 1,988,331 and 1,370,809 reads were monitored in the bacterial and archaeal communities, respectively. There were three dominant archaeal phyla: Euryarchaeota, Crenarchaeota, and Thaumarchaeota in all treatments. At the archaeal order level (relative abundance >1%), six dominating categories were found in all treatments (Fig. 3A). In the control, the abundance of order Bathyarchaeia gradually increased and became dominant throughout the anaerobic incubation. With glucose, the main order was Bathyarchaeia at the initial stage (1 day), changed entirely to the order Methanosarcinales at the middle stage (44 days), and became Methanobacteriales dominant at the later stage (90 days). With starch, the order composition was similar to that of glucose, except that Methanosarcinales and Methanobacteriales dominated on day 44. With acetate, as the culture proceeded, the proportions of Methanosarcinales and Methanobacteriales gradually increased and became dominant by day 90. With nonanoate, the proportion of Methanocellales gradually increased as the incubation progressed. *Methanobacterium* and *Methanosarcina* were the dominant archaea in the glucose and starch treatments at the

Table 1
Correlation analysis for functional genes and physicochemical factors.

	pH	Eh	DOC	MBC	NH_4^+	CH_4	AK	Fe^{2+}	Fe^{3+}
Eh	–	–	–	–	–	–	–	–	–
DOC	0.48***	–	–	–	–	–	–	–	–
MBC	0.48***	–	0.69***	–	–	–	–	–	–
NH_4^+	0.47**	0.68***	0.49***	0.32*	–	–	–	–	–
NO_3^-	–	0.66***	–	–	0.48***	–	–	–	–
CH_4	−0.37*	–	−0.33*	–	–	–	–	–	–
AP	–	–	0.51***	0.45**	–	–	–	–	–
AK	−0.37*	−0.50***	−0.40**	−0.36*	−0.69***	–	–	–	–
Fe^{2+}	−0.68***	–	−0.45**	−0.37*	−0.35*	0.46**	0.54***	–	–
Fe^{3+}	0.83***	−0.31*	0.53***	0.43**	0.50***	−0.49***	−0.56***	−0.92***	–
mcrA	−0.72***	−0.44**	−0.50***	−0.33*	−0.43**	0.58***	0.47**	0.86***	−0.88***
pmoA	0.32*	–	–	–	–	−0.32*	–	–	–

The significant correlation ($P < 0.05$) were shown in this table.
* $P < 0.05$.
** $P < 0.01$.
*** $P < 0.001$.

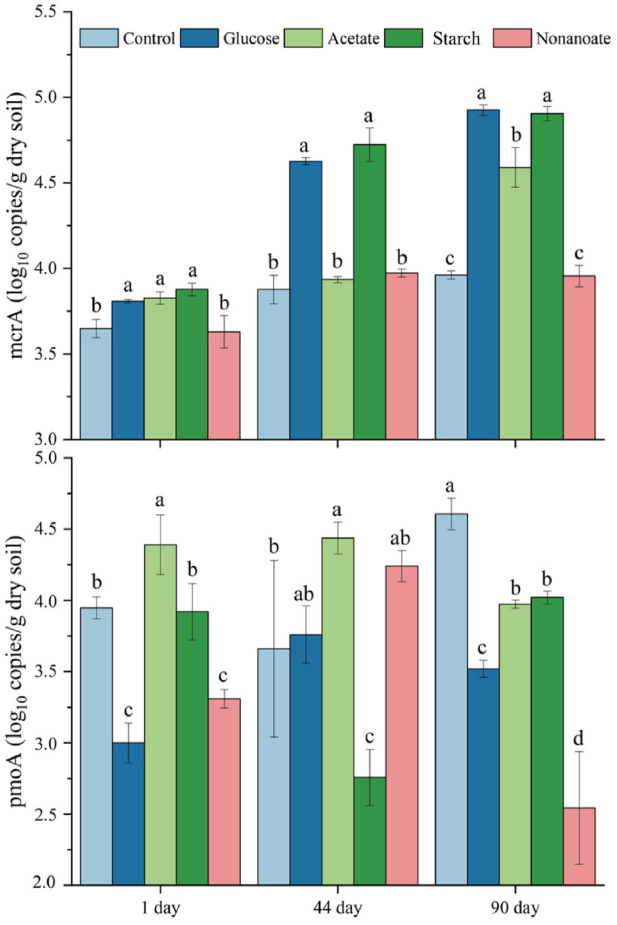

Fig. 2. *McrA* and *pmoA* genes copies with different carbon sources. The error bars show standard error ($n = 3$). Different letters represent significant differences ($P < 0.05$).

taxonomic genus level (Fig. S1). Through the sequencing of the bacteria, we found that the iron-reducing bacteria (*Clostridium* sensu stricto and *Geobacter*) was significantly increased in the glucose and starch treatments (Fig. 3B).

We used alpha diversity (Chao1 diversity and Shannon index) to explore the richness and diversity of each sample (Fig. 4). On days 44, the Chao1 diversity and Shannon index of bacteria and the Chao1 diversity of archaea with glucose and starch treatments decreased significantly compared to the control ($P < 0.05$). The Chao1 diversity and Shannon index of bacteria with the acetate and nonanoate treatments increased significantly compared to the control ($P < 0.05$), and the Chao1 diversity and Shannon index of the archaea with the acetate treatment increased significantly compared to the control ($P < 0.05$). Principal Coordinate of Analysis (PCoA) plot showed the microbial community differences of archaea among the different carbon sources (Fig. 5A). We found the archaeal community structures for all carbon sources were significantly different ($P = 0.001$). The layout of the PCoA plot divided into two areas: the lower right and the upper left. The treatments for CH_4 emissions were located at the lower right (glucose and starch on 44 days; glucose, acetate, and starch on 90 days). However, the treatments with no CH_4 emissions were gathered at the upper left. Furthermore, RDA was used to study the relationship among functional genes, CH_4 emission, physicochemical factors, and methanogenic archaeal communities at the order level (Fig. 5B). The RDA plot displayed 20 environmental and microbial parameters and explained 83.88% of the total variation for the first two axes. From the plot, we observed that the relative abundance of Methanobacteriales was possibly correlated with glucose and starch, and the relative abundance of Methanosarcinales was possibly correlated with acetate. To study the difference in the methanogenic microbiota among the various treatments, the LEfSe method was performed. From the cladogram (Fig. 6), we found 27 biomarkers identified at three different time points. No matter which period we choose, Euryarchaeota contributed to the most significant differences. The microbial taxa showing difference were similar on 44 and 90 days, but different treatments had different microorganisms. The class of Methanobacteria was the most abundant biomarker identified in the control treatment on day 1, and in the starch treatment on days 44 and 90. The class of Thermoplasmata was significantly enriched in the glucose treatment on day 1, in the control treatment on day 44, and in the nonanoate treatment on day 90. The orders of Nitrososphaerales, Methanosaetaceae, Rice_Cluster_II, and Methanosarcinales were abundant in the acetate treatment for the whole culture period. We plotted a heatmap to display the correlation of genus level of archaea (top 15) with physicochemical properties and found *Methanobacterium* and *Methanosarcina* showed a significantly positive correlation with CH_4 emissions ($P < 0.001$) (Fig. 7). We also observed that *Methanosarcina* was closely related to the iron reduction process.

4. Discussion

4.1. CH_4 and CO_2 emission with different carbon sources

Our results showed that the carbon sources glucose and starch have a significant influence on CH_4 production capability, but the addition of acetate produced less methane and much later. The organic acids (other than acetate) produced by the oxidation of glucose are used as substrates for methane production (Horvath et al., 2019), but glucose itself does not produce methane (Vadlani and Ramachandran, 2008). In addition, glucose can be quickly absorbed and converted into various organic acids, mainly lactic acid under anaerobic conditions (Ferguson et al., 2018), and different acids have different methane production capabilities. Related studies have found that the process of interspecies electron transfer promotes the metabolism of butyric acid and benzoic acid to methane (Zhuang et al., 2015). In our study, Fe^{3+} as an electron acceptor may also promote this process and inhibit acetate utilization. Furthermore, glucose is the most abundant carbon source in the soil, and most microorganisms can use glucose as an energy substrate for metabolism (Nazarko et al., 2008). The methanogenic ability of starch is similar to that of glucose, since starch is composed of glucose monomers linked by α-(1,4) glycosidic bonds (Meier et al., 2018).

4.2. *mcrA* and *pmoA* genes with different carbon sources

mcrA and *pmoA* genes have been confirmed to be related to CH_4 metabolism and responsible for the production and oxidation of CH_4, respectively (Freitag et al., 2010). We have found that the *mcrA* gene copy number was positively correlated with CH_4 concentration ($P < 0.001$) in flooded paddy fields, which agrees with other studies (Wang et al., 2018; Jiang et al., 2019). Moreover, during the anaerobic incubation, the copy number of the *mcrA* gene increased significantly with the carbon source treatments glucose, acetate, and starch, which would also be associated with the decomposition of soil organic matter. Methanogens can obtain energy for growth and reproduction by anaerobic degradation of small organic matter to methane (Cai et al., 2019). In addition, we also observed that the copy number of the *mcrA* gene was closely related to pH and iron reduction. This could be explained by recent reports that iron can promote the decomposition of soil organic matter under anaerobic conditions (Chen et al., 2020). Additionally, Chen et al. (2020) suggest that when predicting iron oxide-mediated greenhouse gas emissions from the environment, the critical impact of pH on the entire reaction system should be considered. Our results confirmed that pH could significantly affect the reduction of Fe^{3+} in flooded paddy fields. This result is very similar to the reported by (Marquart et al., 2019), who observed that the reduction of iron decreased by 85% during pH changing from 6 to 7.5. Meanwhile, we found that DOC, as a natural energy substance, influenced soil microbial activity and functional gene diversity (Shen et al., 2016). In our study, a significant negative correlation was detected between DOC concentrations and the abundance

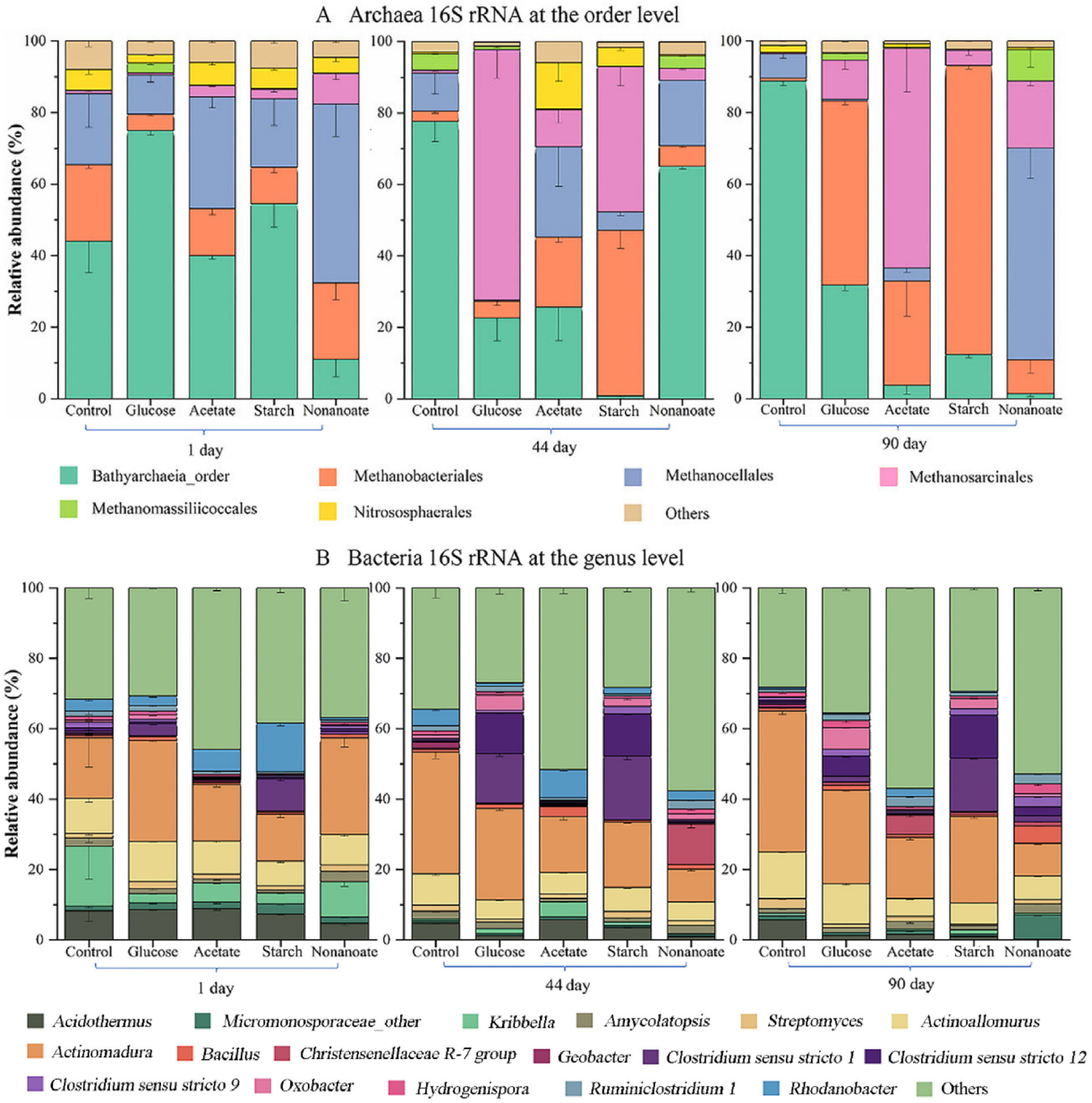

Fig. 3. The community composition of Archaea at the order level (A) and Bacteria at the genus level (B) on days 1, 44, and 90 (Average relative abundance >1%). Data are means ± SD (n = 3).

of *mcrA* at the end of the incubation, suggesting the increase of *mcrA* copies relates to the consumption of DOC. Likewise, the same trend was detected between the *mcrA* gene copy number and the DOC concentrations in paddy fields (Wang et al., 2021). However, some studies have demonstrated that soil DOC can limit the growth of methanogens and promote the utilization of methane by methanotrophs (Bossio et al., 1999; Wang et al., 2020). These findings indicate that CH_4 fluxes might be controlled by the availability of carbon substrates (Seo et al., 2013).

4.3. Methanogenic community structure with different carbon sources

We characterized archaea and bacteria using high-throughput DNA sequencing and the orders of Methanobacteriales and Methanosarcinales were the dominant methanogens with the addition of different carbon sources. These two methanogens orders are dominant in paddy soil, as reported previously (Hernández et al., 2017; Yuan et al., 2018). Generally, methane is formed via hydrogenotrophic, methylotrophic, and acetoclastic pathways. When glucose or starch was used as the carbon source, the dominant methanogen was methylotrophic and acetoclastic Methanosarcinales at the initial stage of incubation (Beckmann et al., 2011), then became Methanobacteriales (hydrogenotrophic methanogenesis) at the later stage of incubation (Yin et al., 2020). The strict anaerobic environment of this experiment provided the optimum conditions for the growth and activity of methanogens. *Methanobacterium* and *Methanosarcina* were detected as the prominent methanogens at the genus level. Methane production began at the later stage of incubation in the acetate treatment, and the main methanogen was detected as *Methanosarcina*, which was also found to be enriched on acetate from Italian paddy soil (Fetzer et al., 1993). *Methanobacterium* and *Methanosarcina* were dominant in the glucose and starch treatments and positively correlated with CH_4 emissions (Fig. S1 and Fig. 7), which is consistent with the result that CH_4 emissions mainly occurred with the glucose and starch treatments (Fig. 1).

This study showed a significant negative correlation between Fe^{3+} concentration and CH_4 emission ($P < 0.001$), and the iron-reducing bacteria (*Geobacter*, *Clostridium* sensu stricto) were enriched mainly in the glucose and starch treatments. This may be because the glucose serves as an

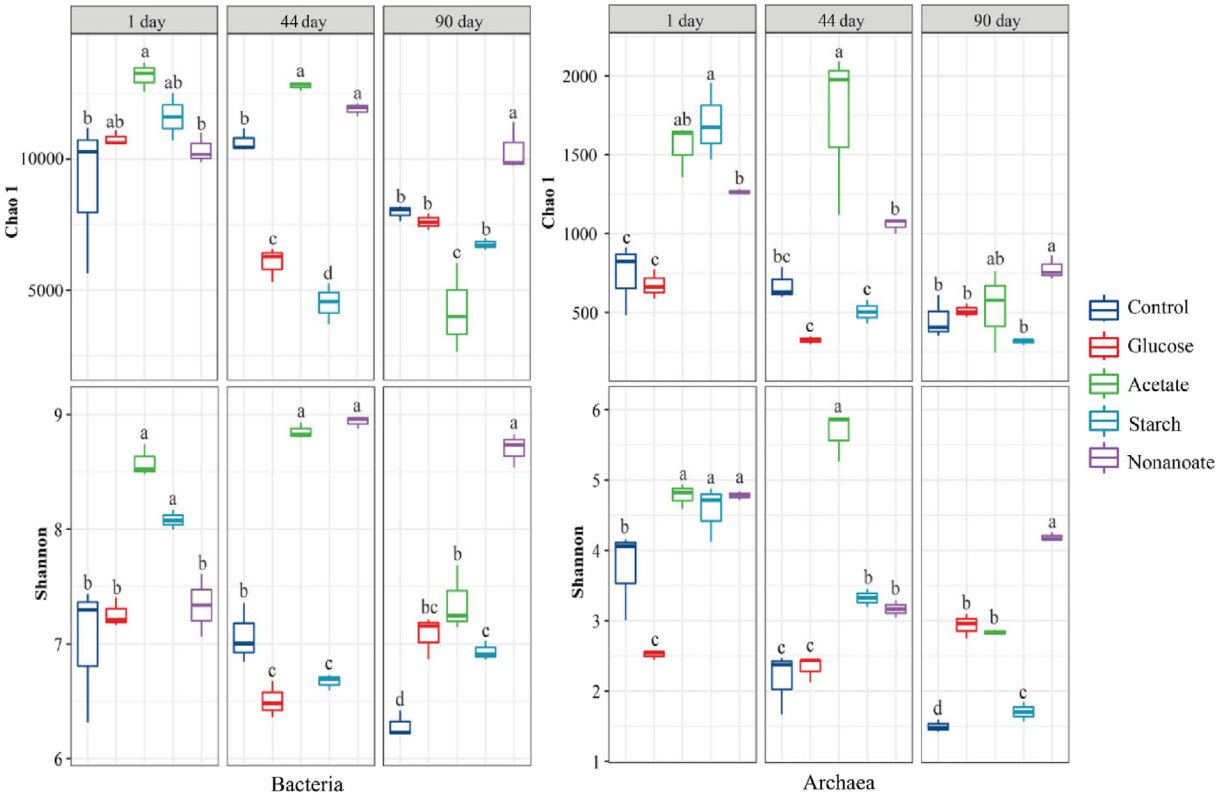

Fig. 4. Boxplot of alpha-diversity analyses (Chao1 richness and Shannon index) of Bacteria and Archaea. Data are means ± SD (n = 3).

electron donor facilitating the binding of the electron acceptor (Fe^{3+}). Similarly, iron-reducing bacteria can couple to the oxidation of organic carbon and obtain energy to maintain their own metabolism (Liu et al., 2015). Rotaru et al. (2014) found that the co-cultures of *Geobacter metallireducens* (iron-reducing bacteria) and *Methanosaeta harundinacea* (methanogen) further enhanced DIET and the reduction of CO_2 to CH_4. Likewise, Liu et al. (2010) found the addition of glucose could facilitate the reduction of Cr (VI) due to its ability to be an electron donor. Similarly, Kwon et al. (2011) added 2 mM acetate to aquifer sediment and found the reduction of Fe^{3+} was significantly enhanced. Therefore, carbon sources serve as electron donors with different abilities to couple to terminal electron acceptors in different habitats. Fe^{3+} is the most abundant mineral oxide in paddy soil and plays an important role in the storage and stability of SOC (Porras et al., 2017; Luo et al., 2021). We found the order of Methanobacteriales and the genus of *Methanosarcina* gave a significant correlation with Fe^{2+} concentration. Interestingly, Zhang et al. (2012) reported that *Methanosarcina mazei*, a mesophilic methanogen, could reduce Fe^{3+} to Fe^{2+}. All these suggest that DIET between cometabolism microbes of iron-reducing bacteria and methanogens plays a key role in the anaerobic methanogenesis.

This study was performed in a laboratory setting. However, the changes in methanogens and iron-reducing bacteria in iron-mediated paddy soil should be further verified by carrying out in-situ experiments. Moreover, the anaerobic methane oxidation process is a crucial player for reducing CH_4 emissions. While we only evaluated the methanogenic process and

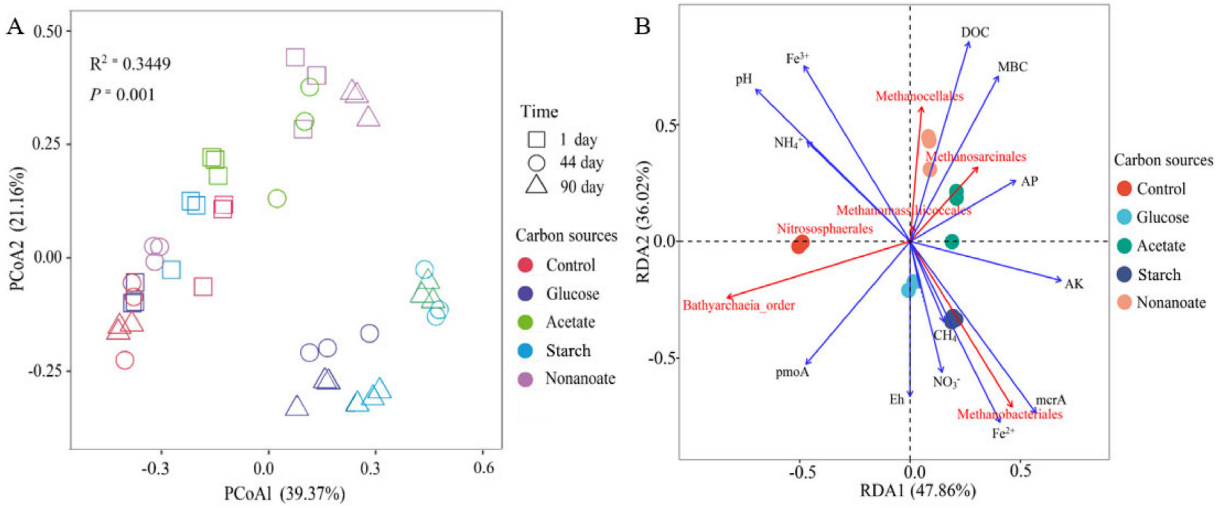

Fig. 5. Principal Coordinate Analysis (PCoA) of different carbon sources on days 1, 44, and 90 (A), and redundancy analysis (RDA) displaying the relationship among functional genes, CH_4 emission, and physicochemical factors on day 90 (B).

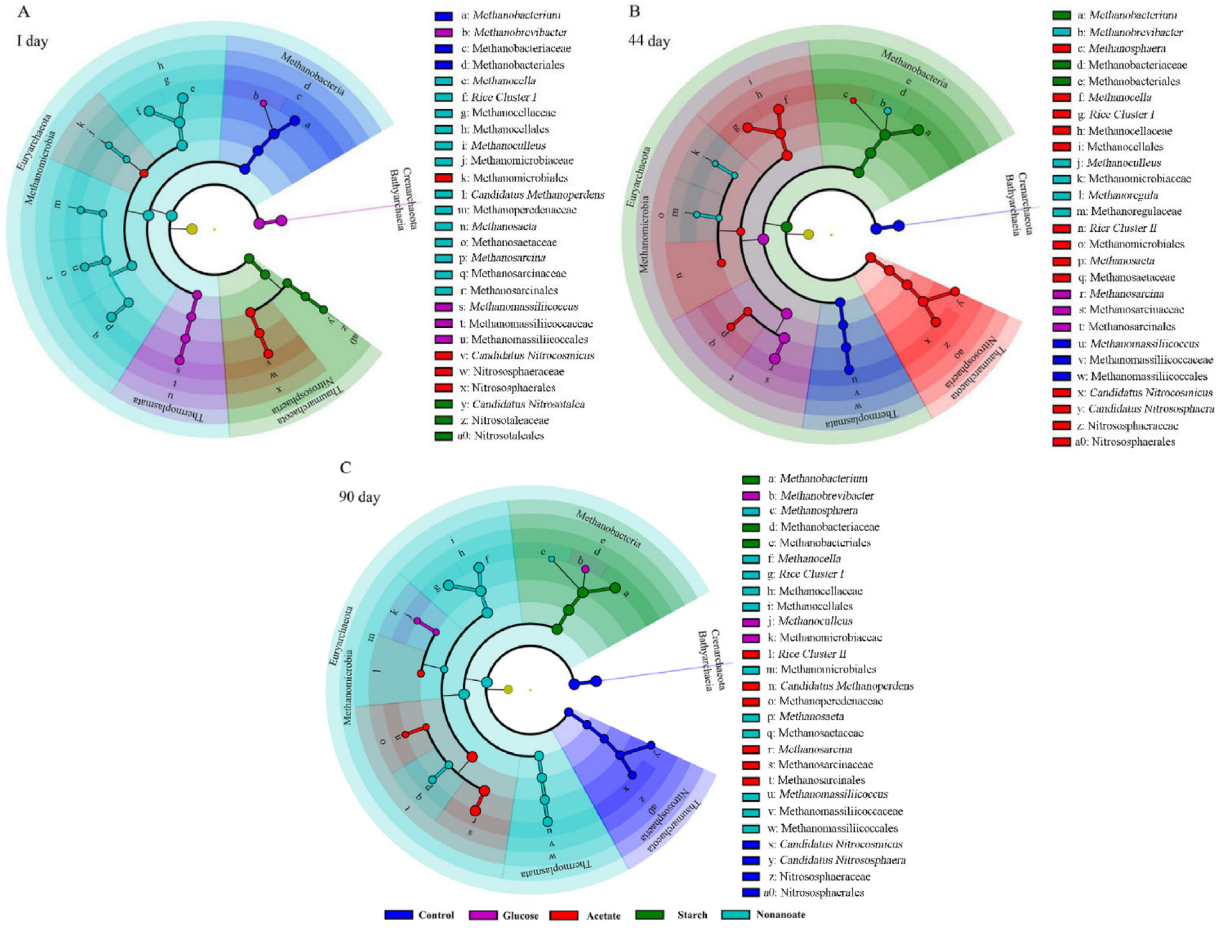

Fig. 6. Archaeal biomarkers among different treatments at three distinct periods by the analysis of the LEfSe.

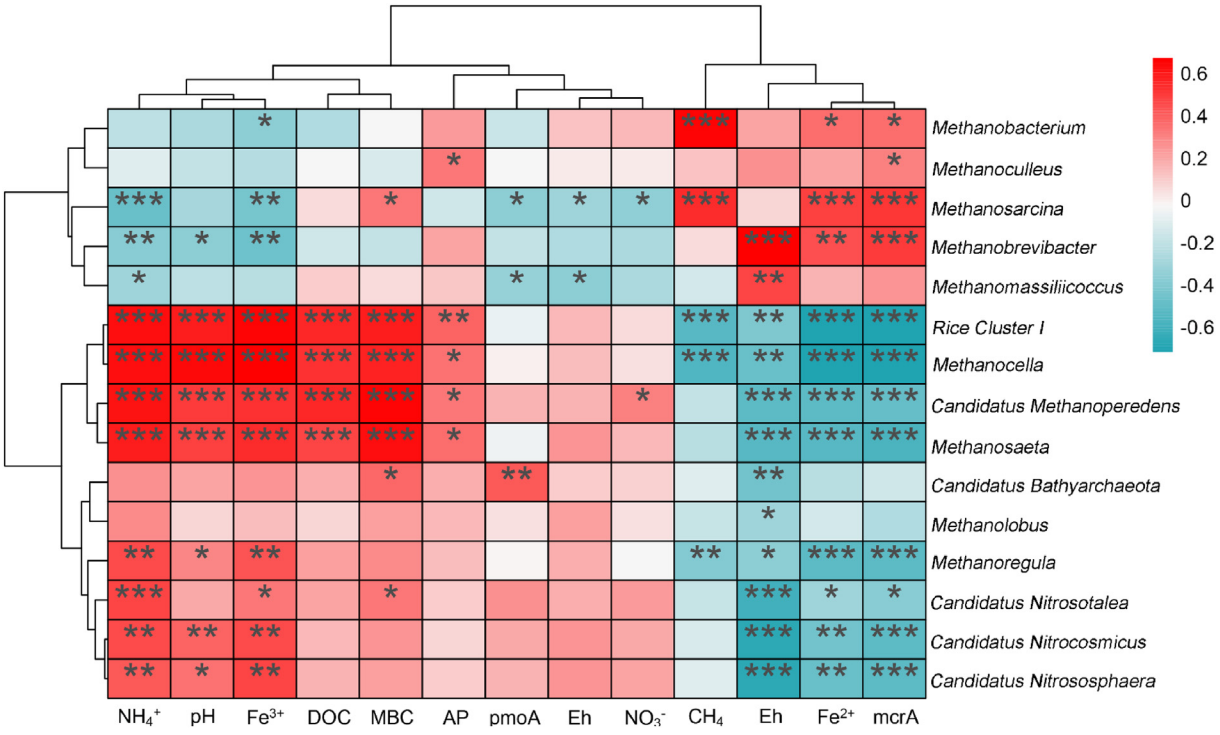

Fig. 7. Hierarchical clustering heatmap of the genus level of Archaea (top 15) and functional genes, CH_4 emission, and physicochemical properties based on the Pearson correlation. * $P < 0.05$; ** $P < 0.01$; *** $P < 0.001$.

the capacity of CH_4 production with different carbon sources, this can also be explored to assist in mitigating CH_4 emissions from paddy soil. We found the number of iron-reducing bacteria and the content of CH_4 were significantly increased in the glucose and starch treatments. Whether that is because glucose acts as an electron donor to reduce iron or the regulation of the iron reduction process on CH_4 production is involved is unclear. Further studies are required to investigate this issue. In addition, whether the iron reduction process affects CH_4 emissions by changing soil organic matter characteristics or electron transfer processes will need to be studied in the future.

5. Conclusion

The methane production rate differed with several carbon sources from flooded paddy soil. Glucose and starch with higher methane production rates than acetate, and acetate has a certain degree of delay in reaction time, and nonanoate, as a higher carbon chain length substrate, cannot play a role in methane production. Glucose and starch can produce methane through a series of reactions and the main related methanogens are Methanosarcinales and Methanobacteriales. In contrast, the dominant methanogen is Methanosarcinales under acetate amendment condition. The anaerobic incubation time influences the composition and abundance of methanogenic communities but has no obvious effect on bacterial communities. Notably, the iron reduction process and pH are significantly correlated with the methanogenic gene (*mcrA*) and methane production, and suggested the role of ferric oxides and pH should be considered when involved in methane emission from flooded paddy soil.

Supplementary data to this article can be found online at https://doi.org/10.1016/j.scitotenv.2022.153636.

CRediT authorship contribution statement

Dan Luo: Conceptualization, Methodology, Software, Data curation, Validation, Writing – original draft, Visualization, Investigation, Writing – review & editing. **Yaying Li:** Conceptualization, Data curation, Validation, Writing – review & editing. **Huaiying Yao:** Conceptualization, Methodology, Software, Data curation, Validation, Writing – review & editing, Supervision, Funding acquisition. **Stephen J. Chapman:** Conceptualization, Writing – review & editing.

Declaration of competing interest

The authors declare that they have no known competing financial interests or personal relationships that could have appeared to influence the work reported in this paper.

Acknowledgements

This work was supported by the National Natural Science Foundation of China [Grant Numbers 42077036, 42021005], the National Key R & D Program of China [Grant Number 2020YFC1806900], and Ningbo Municipal Science and Technology Bureau (202002N3079).

References

Achtnich, C., Bak, F., Conrad, R., 1995. Competition for electron donors among nitrate reducers, ferric iron reducers, sulfate reducers, and methanogens in anoxic paddy soil. Biol. Fert. Soils 19 (1), 65–72.

Bachoon, D., Jones, R.D., 1992. Potential rates of methanogenesis in sawgrass marshes with peat and marl soils in the everglades. Soil Biol. Biochem. 24 (1), 21–27.

Beckmann, S., Lueders, T., Krüger, M., von Netzer, F., Engelen, B., Cypionka, H., 2011. Acetogens and acetoclastic methanosarcinales govern methane formation in abandoned coal mines. Appl. Environ. Microb. 77 (11), 3749.

Borrel, G., Parisot, N., Harris, H.M.B., Peyretaillade, E., Gaci, N., Tottey, W., Bardot, O., Raymann, K., Gribaldo, S., Peyret, P., O'Toole, P.W., Brugère, J., 2014. Comparative genomics highlights the unique biology of methanomassiliicoccales, a thermoplasmatales-related seventh order of methanogenic archaea that encodes pyrrolysine. BMC Genomics 15, 679.

Bossio, D.A., Horwath, W.R., Mutters, R.G., van Kessel, C., 1999. Methane pool and flux dynamics in a rice field following straw incorporation. Soil Biol. Biochem. 31 (9), 1313–1322.

Bridgham, S.D., Richardson, C.J., 1992. Mechanisms controlling soil respiration (CO_2 and CH_4) in southern peatlands. Soil Biol. Biochem. 24 (11), 1089–1099.

Bryce, C., Franz-Wachtel, M., Nalpas, N.C., Miot, J., Benzerara, K., Byrne, J.M., Kleindienst, S., Macek, B., Kappler, A., Müller, V., 2018. Proteome response of a metabolically flexible anoxygenic phototroph to Fe(II) oxidation. Appl. Environ. Microb. 84 (16), e1118–e1166.

Cai, P., Ning, Z., Zhang, N., Zhang, M., Guo, C., Niu, M., Shi, J., 2019. Insights into biodegradation related metabolism in an abnormally low dissolved inorganic carbon (DIC) petroleum-contaminated aquifer by metagenomics analysis. Microorganisms 7 (10), 412.

Caporaso, J.G., Lauber, C.L., Walters, W.A., Berg-Lyons, D., Lozupone, C.A., Turnbaugh, P.J., Fierer, N., Knight, R., 2011. Global patterns of 16S rRNA diversity at a depth of millions of sequences per sample. Proc. Natl. Acad. Sci. USA 108 (Suppl. 1), 4516–4522.

Chen, C., Hall, S.J., Coward, E., Thompson, A., 2020. Iron-mediated organic matter decomposition in humid soils can counteract protection. Nat. Commun. 11 (1), 2255.

Crouch, S.R., Malmstadt, H.V., 1967. Mechanistic investigation of molybdenum blue method for determination of phosphate. Anal. Chem. 39 (10), 1084–1089.

Edgar, R.C., 2013. UPARSE: highly accurate OTU sequences from microbial amplicon reads. Nat. Methods 10 (10), 996–998.

Ferguson, B.S., Rogatzki, M.J., Goodwin, M.L., Kane, D.A., Rightmire, Z., Gladden, L.B., 2018. Lactate metabolism: historical context, prior misinterpretations, and current understanding. Eur. J. Appl. Physiol. 118 (4), 691–728.

Fetzer, S., Bak, F., Conrad, R., 1993. Sensitivity of methanogenic bacteria from paddy soil to oxygen and desiccation. FEMS Microbiol. Ecol. 12 (2), 107–115.

Freitag, T.E., Toet, S., Ineson, P., Prosser, J.I., 2010. Links between methane flux and transcriptional activities of methanogens and methane oxidizers in a blanket peat bog. FEMS Microbiol. Ecol. 73 (1), 157–165.

Fu, L., Lu, Y., Tang, L., Hu, Y., Xie, Q., Zhong, L., Fan, C., Liu, Q., Zhang, S., 2021. Dynamics of methane emission and archaeal microbial community in paddy soil amended with different types of biochar. Appl. Soil Ecol. 162, 103892.

Guérin, F., Abril, G., de Junet, A., Bonnet, M., 2008. Anaerobic decomposition of tropical soils and plant material: implication for the CO_2 and CH_4 budget of the petit saut reservoir. Appl. Geochem. 23 (8), 2272–2283.

Gütlein, A., Gerschlauer, F., Kikoti, I., Kiese, R., 2018. Impacts of climate and land use on N_2O and CH_4 fluxes from tropical ecosystems in the Mt. Kilimanjaro region, Tanzania. Glob. Chang. Biol. 24 (3), 1239–1255.

Gwon, H.S., Khan, M.I., Alam, M.A., Das, S., Kim, P.J., 2018. Environmental risk assessment of steel-making slags and the potential use of LD slag in mitigating methane emissions and the grain arsenic level in rice (*Oryza sativa* L.). J. Hazard. Mater. 353, 236–243.

Hanke, A., Cerli, C., Muhr, J., Borken, W., Kalbitz, K., 2013. Redox control on carbon mineralization and dissolved organic matter along a chronosequence of paddy soils. Eur. J. Soil Sci. 64 (4), 476–487.

Hernández, M., Conrad, R., Klose, M., Ma, K., Lu, Y., 2017. Structure and function of methanogenic microbial communities in soils from flooded rice and upland soybean fields from Sanjiang Plain, NE China. Soil Biol. Biochem. 105, 81–91.

Horvath, N., Vilkhovoy, M., Wayman, J.A., Calhoun, K., Swartz, J., Varner, J.D., 2019. Toward a genome scale sequence specific dynamic model of cell-free protein synthesis in *Escherichia coli*. Metab. Eng. Commun. 10, e113.

Jiang, J., Wang, Y., Liu, J., Yang, X., Ren, Y., Miao, H., Pan, Y., Lv, J., Yan, G., Ding, L., Li, Y., 2019. Exploring the mechanisms of organic matter degradation and methane emission during sewage sludge composting with added vesuvianite: insights into the prediction of microbial metabolic function and enzymatic activity. Bioresour. Technol. 286, 121397.

Kosugi, Y., Matsuura, N., Liang, Q., Yamamoto-Ikemoto, R., 2020. Wastewater treatment using the "sulfate reduction, denitrification anammox and partial nitrification (SRDAPN)" process. Chemosphere 256, 127092.

Kwon, M.J., O Loughlin, E.J., Antonopoulos, D.A., Finneran, K.T., 2011. Geochemical and microbiological processes contributing to the transformation of hexahydro-1,3,5-trinitro-1,3,5-triazine (RDX) in contaminated aquifer material. Chemosphere 84 (9), 1223–1230.

Lanquar, V., Lelièvre, F., Bolte, S., Hamès, C., Alcon, C., Neumann, D., Vansuyt, G., Curie, C., Schröder, A., Krämer, U., Barbier-Brygoo, H., Thomine, S., 2005. Mobilization of vacuolar iron by AtNRAMP3 and AtNRAMP4 is essential for seed germination on low iron. EMBO J. 24 (23), 4041–4051.

Lazcano, C., Gómez-Brandón, M., Domínguez, J., 2008. Comparison of the effectiveness of composting and vermicomposting for the biological stabilization of cattle manure. Chemosphere 72 (7), 1013–1019.

Liechty, Z., Santos-Medellín, C., Edwards, J., Nguyen, B., Mikhail, D., Eason, S., Phillips, G., Sundaresan, V., 2020. Comparative analysis of root microbiomes of rice cultivars with high and low methane emissions reveals differences in abundance of methanogenic archaea and putative upstream fermenters. mSystems 5 (1), e819–e897.

Liu, Y., Whitman, W.B., 2008. Metabolic, phylogenetic, and ecological diversity of the methanogenic archaea. Ann. N. Y. Acad. Sci. 1125 (1), 171–189.

Liu, G., Yang, H., Wang, J., Jin, R., Zhou, J., Lv, H., 2010. Enhanced chromate reduction by resting *Escherichia coli* cells in the presence of quinone redox mediators. Bioresour. Technol. 101 (21), 8127–8131.

Liu, Y., Zhang, Y., Ni, B., 2015. Evaluating enhanced sulfate reduction and optimized volatile fatty acids (VFA) composition in anaerobic reactor by Fe(III) addition. Environ. Sci. Technol. 49 (4), 2123–2131.

Liu, C., Li, H., Zhang, Y., Si, D., Chen, Q., 2016. Evolution of microbial community along with increasing solid concentration during high-solids anaerobic digestion of sewage sludge. Bioresour. Technol. 216, 87–94.

Lovley, D.R., Holmes, D.E., Nevin, K.P., 2004. Dissimilatory Fe(III) and Mn(IV) reduction. Advances in Microbial Physiology. Academic Press, pp. 219–286.

Luesken, F.A., Zhu, B., van Alen, T.A., Butler, M.K., Diaz, M.R., Song, B., Op Den Camp, H.J.M., Jetten, M.S.M., Ettwig, K.F., 2011. pmoA primers for detection of anaerobic methanotrophs. Appl. Environ. Microb. 77 (11), 3877–3880.

Luo, D., Meng, X., Zheng, N., Li, Y., Yao, H., Chapman, S.J., 2021. The anaerobic oxidation of methane in paddy soil by ferric iron and nitrate, and the microbial communities involved. Sci. Total Environ. 788, 147773.

Marquart, K.A., Haller, B.R., Paper, J.M., Flynn, T.M., Boyanov, M.I., Shodunke, G., Gura, C., Jin, Q., Kirk, M.F., 2019. Influence of pH on the balance between methanogenesis and iron reduction. Geobiology 17 (2), 185–198.

Meier, K.K., Jones, S.M., Kaper, T., Hansson, H., Koetsier, M.J., Karkehabadi, S., Solomon, E.I., Sandgren, M., Kelemen, B., 2018. Oxygen activation by Cu LPMOs in recalcitrant carbohydrate polysaccharide conversion to monomer sugars. Chem. Rev. 118 (5), 2593–2635.

Nan, Q., Wang, C., Wang, H., Yi, Q., Wu, W., 2020. Mitigating methane emission via annual biochar amendment pyrolyzed with rice straw from the same paddy field. Sci. Total Environ. 746, 141351.

Nazarko, V.Y., Futej, K.O., Thevelein, J.M., Sibirny, A.A., 2008. Differences in glucose sensing and signaling for pexophagy between the baker's yeast *Saccharomyces cerevisiae* and the methylotrophic yeast Pichia pastoris. Autophagy 4 (3), 381–384.

Pachauri, R.K., Allen, M.R., Barros, V.R., Broome, J., Cramer, W., Christ, R., Church, J.A., Clarke, L., Dahe, Q., Dasgupta, P., 2014. Climate change 2014: synthesis report. Contribution of Working Groups I, II and III to the fifth assessment report of the Intergovernmental Panel on Climate Change. IPCC.

Peng, Q., Shaaban, M., Hu, R., Mo, Y., Wu, Y., Ullah, B., 2015. Effects of soluble organic carbon addition on CH_4 and CO_2 emissions from paddy soils regulated by iron reduction processes. Soil Res. 53 (3), 316–324.

Porras, R.C., Hicks Pries, C.E., McFarlane, K.J., Hanson, P.J., Torn, M.S., 2017. Association with pedogenic iron and aluminum: effects on soil organic carbon storage and stability in four temperate forest soils. Biogeochemistry 133 (3), 333–345.

Quast, C., Pruesse, E., Yilmaz, P., Gerken, J., Schweer, T., Yarza, P., Peplies, J., Glöckner, F.O., 2012. The SILVA ribosomal RNA gene database project: improved data processing and web-based tools. Nucleic Acids Res. 41 (D1), D590–D596.

Rago, L., Ruiz, Y., Baeza, J.A., Guisasola, A., Cortés, P., 2015. Microbial community analysis in a long-term membrane-less microbial electrolysis cell with hydrogen and methane production. Bioelectrochemistry 106, 359–368.

Rotaru, A., Shrestha, P.M., Liu, F., Shrestha, M., Shrestha, D., Embree, M., Zengler, K., Wardman, C., Nevin, K.P., Lovley, D.R., 2014. A new model for electron flow during anaerobic digestion: direct interspecies electron transfer to methanosaeta for the reduction of carbon dioxide to methane. Energy Environ. Sci. 7 (1), 408–415.

Segata, N., Izard, J., Waldron, L., Gevers, D., Miropolsky, L., Garrett, W.S., Huttenhower, C., 2011. Metagenomic biomarker discovery and explanation. Genome Biol. 12 (6), R60.

Seo, M., Kim, A., Kim, S., 2013. Environmental and economic impacts of transit-oriented corridors in Korea. J. Asian Archit. Build. 12 (2), 213–220.

Shen, C., Shi, Y., Ni, Y., Deng, Y., Van Nostrand, J.D., He, Z., Zhou, J., Chu, H., 2016. Dramatic increases of soil microbial functional gene diversity at the treeline ecotone of Changbai Mountain. Front. Microbiol. 7, 1184.

Su, J., Hu, C., Yan, X., Jin, Y., Chen, Z., Guan, Q., Wang, Y., Zhong, D., Jansson, C., Wang, F., Schnürer, A., Sun, C., 2015. Expression of barley SUSIBA2 transcription factor yields high-starch low-methane rice. Nature 523 (7562), 602–606.

Summers, Z.M., Fogarty, H.E., Leang, C., Franks, A.E., Malvankar, N.S., Lovley, D.R., 2010. Direct exchange of electrons within aggregates of an evolved syntrophic coculture of anaerobic bacteria. Science 330 (6009), 1413–1415.

Vadlani, P.V., Ramachandran, K.B., 2008. Evaluation of UASB reactor performance during start-up operation using synthetic mixed-acid waste. Bioresource Technol. 99 (17), 8231–8236.

Vaksmaa, A., Jetten, M.S.M., Ettwig, K.F., Lüke, C., 2017. McrA primers for the detection and quantification of the anaerobic archaeal methanotroph '*Candidatus methanoperedens nitroreducens*'. Appl. Microbiol. Biot. 101 (4), 1631–1641.

Vance, E.D., Brookes, P.C., Jenkinson, D.S., 1987. An extraction method for measuring soil microbial biomass C. Soil Biol. Biochem. 19 (6), 703–707.

Wandersman, C., Delepelaire, P., 2004. Bacterial iron sources: from siderophores to hemophores. Annu. Rev. Microbiol. 58 (1), 611–647.

Wang, Y., Bai, R., Di, H.J., Mo, L., Han, B., Zhang, L., He, J., 2018. Differentiated mechanisms of biochar mitigating straw-induced greenhouse gas emissions in two contrasting paddy soils. Front. Microbiol. 9, 2566.

Wang, L., Qin, T., Liu, T., Guo, L., Li, C., Zhai, Z., 2020. Inclusion of microbial inoculants with straw mulch enhances grain yields from rice fields in Central China. Food Energy Secur. 9 (4), e230.

Wang, Y., Hu, Z., Shen, L., Liu, C., Islam, A.R.M.T., Wu, Z., Dang, H., Chen, S., 2021. The process of methanogenesis in paddy fields under different elevated CO_2 concentrations. Sci. Total Environ. 773, 145629.

Weber, K.A., Achenbach, L.A., Coates, J.D., 2006. Microorganisms pumping iron: anaerobic microbial iron oxidation and reduction. Nat. Rev. Microbiol. 4 (10), 752–764.

Xu, S., Zhang, W., Zuo, L., Qiao, Z., He, P., 2020b. Comparative facilitation of activated carbon and goethite on methanogenesis from volatile fatty acids. Bioresource Technol. 302, 122801.

Xu, Y., Zhang, L., Ou, S., Wang, R., Wang, Y., Chu, C., Yao, S., 2020a. Natural variations of SLG1 confer high-temperature tolerance in indica rice. Nat. Commun. 11 (1), 5441.

Yin, Q., Gu, M., Hermanowicz, S.W., Hu, H., Wu, G., 2020. Potential interactions between syntrophic bacteria and methanogens via type IV pili and quorum-sensing systems. Environ. Int. 138, 105650.

Yuan, Q., Hernández, M., Dumont, M.G., Rui, J., Fernández Scavino, A., Conrad, R., 2018. Soil bacterial community mediates the effect of plant material on methanogenic decomposition of soil organic matter. Soil Biol. Biochem. 116, 99–109.

Zhang, J., Dong, H., Liu, D., Fischer, T.B., Wang, S., Huang, L., 2012. Microbial reduction of Fe(III) in illite–smectite minerals by methanogen *Methanosarcina mazei*. Chem. Geol. 292–293, 35–44.

Zhuang, L., Tang, J., Wang, Y., Hu, M., Zhou, S., 2015. Conductive iron oxide minerals accelerate syntrophic cooperation in methanogenic benzoate degradation. J. Hazard. Mater. 293, 37–45.